Title
Thin film nanocalorimeter for heat capacity measurements of 30 nm films.

Journal
The Review of scientific instruments, 80(6)

ISSN
0034-6748

Authors
Queen, DR
Hellman, F

Publication Date
2009-06-01

DOI
10.1063/1.3142463

Peer reviewed

Thin film nanocalorimeter for heat capacity measurements of 30 nm films

D. R. Queen[a] and F. Hellman
Department of Physics, University of California, Berkeley, Berkeley, California 94720, USA

(Received 27 February 2009; accepted 1 May 2009; published online 1 June 2009)

A silicon nitride membrane-based nanocalorimeter is described for measuring the heat capacity of 30 nm films from 300 mK to 800 K and in high magnetic fields with absolute accuracy ~2%. The addenda heat capacity of the nanocalorimeter is less than 2×10^{-7} J/K at room temperature and 2×10^{-10} J/K at 2.3 K. This is more than ten times smaller than any existing calorimeter suitable for measuring thin films over this wide temperature range. The heat capacities of thin Cu and Au films are reported and agree with bulk values. The thermal conductivity of the thin low stress silicon nitride is substantially smaller than thicker membranes while the specific heat is enhanced below 20 K. Design of the nanocalorimeter will be discussed along with fabrication details and calibration results. © *2009 American Institute of Physics.* [DOI: 10.1063/1.3142463]

I. INTRODUCTION

Understanding the thermodynamic properties of nanoscale materials has become increasingly important as samples with nanometer length scales are routinely produced in the laboratory and semiconductor processing technologies shrink to tens of nanometers in size. Heat capacity in particular reveals information about electronic, magnetic, and structural properties. Measurements at the lowest temperatures tell us about the fundamental excitations in a system while measurements to several hundred degrees centigrade are typically most important in revealing phase transitions or determinations of total enthalpy and entropy. Many of these materials (e.g., amorphous, multilayers, and nanostructured) cannot be produced as bulk samples and are not amenable to traditional measurement techniques. Calorimetry measurements necessarily require that the heat capacity of the calorimeter be measured along with the sample of interest. Heat capacity c is an extensive quantity and a calorimeter suitable for measuring these small quantities should have a heat capacity, and thus, of comparable magnitude to the nanoscale materials and films in addition to operating over a wide range of temperatures and fields.

Microcalorimeters based on amorphous, low stress silicon nitride (Si–N) membranes have been used for over a decade to understand the thermodynamics of thin films and small (micrograms) samples.[1–5] Heats of fusion and heat capacities of ultrathin films and monolayers have previously been measured, but these measurements have been confined to high temperatures and zero magnetic field.[6,7] Films as thin as 200 nm have been measured from 2–800 K and in magnetic fields up to 8 T with an absolute accuracy ~2%. (See Ref. 8 and the references therein.)

Here we describe the design and fabrication of a thin film nanocalorimeter for use from 300 mK to 800 K and in high magnetic fields. This nanocalorimeter is a scaled down version of the previously reported microcalorimeter[1,8] and has more than ten times less addenda heat capacity over this wide temperature range, enabling the heat capacities of 30 nm films or submicrogram samples to be measured with ~2% absolute accuracy.[5,9] Calibration measurements for the device will be discussed along with an analysis of the specific heat and thermal conductivity of the amorphous Si–N membrane.

II. DEVICE DESCRIPTION

The low thermal conductance and heat capacity of amorphous Si–N membranes make them ideal for thin film calorimeters both because of their intrinsic properties (high Debye temperature and corresponding low C) and their mechanical strength (can be made extremely thin with a large area).[1,10] These membranes are made from a low stress, silicon rich film that is grown by low pressure chemical vapor deposition (LPCVD) and they are commonly used for x-ray and TEM windows.[11]

Figure 1 shows a schematic (a) and cross section (b) of the new nanocalorimeter with the sample heaters and thermometers labeled. All of the elements on the device are lithographically patterned and their geometries are well known. The 2 mm × 2 mm × 30 nm Si–N membrane acts both as a substrate for the thin film sample and a weak thermal link between the sample and the Si frame. Samples are deposited onto the backside of the membrane in the 1×1 mm^2 sample area through a microfabricated deposition mask, shown in Fig. 1(b). A Cu or Au thermal conduction layer is also deposited on the back of the membrane in the same central sample area to ensure that the sample is isothermal with the thermometers.[9] The sample heater is used to raise the temperature of the sample area from fractions of a degree to several hundred degrees above the frame temperature depending on the measurement technique.

The heat capacities of the membrane, thermal conduction layer, and sample, when present, are the dominant contributions to the total measured heat capacity c_T. The background, or addenda, heat capacity of the calorimeter c_a is due to the membrane, conduction layer, and thin film heaters and

[a]Electronic mail: dqueen@berkeley.edu.

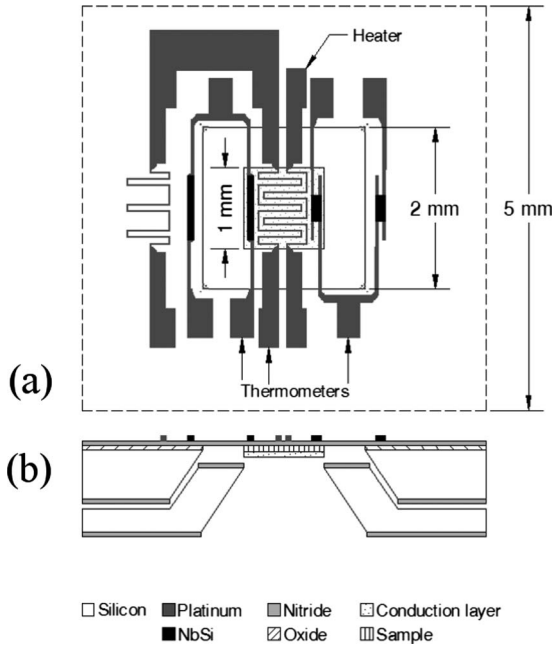

FIG. 1. Schematic of the nanocalorimeter. (a) The sample and conduction layer are in the 1×1 mm^2 square at the center of the 2×2 mm^2 membrane. The silicon chip is 5×5 mm^2. Three sample thermometers (two a-Nb_ySi_{1-y} and one Pt) are located on the sample area with impedance matched thermometers on the frame. Each thermometer's resistance is optimized for a different temperature range. A Pt sample heater is used for all T_0 to heat the sample area with respect to the frame. Lead resistances are $<2\%$ of the measured resistance for the heater and over the range of each thermometer. The Pt heater and thermometer are 12 μm wide. The a-Nb_ySi_{1-y} thermometers have the same doping y and resistances that differ by a factor of 12.5 due to geometry. (b) The 30–50 nm thick low stress, amorphous Si–N membrane is released by etching the Si wafer in KOH and then removing the 100 nm oxide layer in buffered HF. The 10–20 nm thick Pt film is lithographically patterned and etched prior to releasing the membrane. a-Nb_ySi_{1-y} is deposited on the wafer with released membranes, patterned, and then etched. The sample is patterned in the center of the membrane by depositing the film through a separately micromachined deposition mask.

thermometers. The thermal link K that couples the sample area to the environment includes contributions from thermal conduction and radiation. The thermal conduction term depends on the elements that connect the sample area and the frame: Si–N membrane and Pt leads for the heater and thermometers. Heat loss due to radiation becomes appreciable above 100 K and depends on the membrane area and emissivity.[12]

The ability to reliably make thin membranes with a large area sets the minimum possible size for the calorimeter. Here we describe how the important device properties should scale in terms of the device parameters: membrane thickness t and width x. In scaling down the microcalorimeter to reduce c_a, the membrane's strength is kept relatively constant by maintaining the ratio of membrane area to thickness $x^2/t\approx$constant.[11] Membranes as thin as 30 nm are strong enough to withstand fabrication, processing, and routine handling. To meet this constraint for a 30 nm membrane, where t is reduced by a factor of six compared to the 180 nm membrane of the microcalorimeter, the membrane area must be reduced by 6, hence from 5×5 mm^2 to 2×2 mm^2, therefore reducing x by 2.5.

The reduced size of the nanocalorimeter changes two thermodynamic quantities that in turn control all the other measurement parameters: the addenda heat capacity c_a and the thermal link K connecting the sample to the environment. c_a scales in a straight forward manner as it depends only on the total mass $m=\rho V$ of the elements on the membrane. The membrane contribution scales as x^2t and is reduced by a factor of 36 for a 2 mm$\times$2 mm$\times$30 nm membrane. The in-plane dimensions of the heater, thermometers, and leads were reduced by the factor as x and their thicknesses by t_i. If the scaling of $t_i\propto t$, then the overall $c_a\propto x^2t$ which is reduced by a factor of 36. K has contributions from conduction through the membrane and the Pt leads and, for $T>100$ K, a measurable contribution from radiation. Since the device is scaled uniformly in the plane of the wafer, all contributions from conduction scale as $t_i\propto t$. (x appears in both the numerator and denominator of k, hence, is canceled.) The radiation contribution $K_{\mathrm{rad}}=\sigma\epsilon AT^3$ depends on the heated area of the membrane $A\propto x^2\propto t$. Therefore, $K\propto t$ since both contributions separately scale as t. Thus, the heat capacity of films as thin as 30 nm can be measured by scaling the microcalorimeter's membrane thickness t by 6 and area x^2 by 6 to decrease c_a. Furthermore, this scaling results in no change in systematic error for this measurement since the systematic error depends on the ratio of the thermal conductances of conduction layer and membrane which both scale at t.[8]

The measurement sensitivity is determined by the off-null voltage of the bridge circuit $\Delta V=I_{\mathrm{th}}\Delta R$ where I_{th} is the current through the sample thermometer and $\Delta R=\Delta T(dR/dT)$ is the change in thermometer resistance upon heating the sample area. The reduction in t and x for the heaters and thermometers results in an increase in their resistance that scales as t^{-1}. (since all elements' lengths and widths scale as x) The sensitivity of the scaled thermometers is evaluated by considering the bridge response as the relevant figure of merit (FOM). It is shown in Ref. 13 that $\mathrm{FOM}=(t/t_{\mathrm{th}})^{1/2}T^{3/2}/\rho^{1/2}\mathrm{d}\rho/\mathrm{d}T$ where t and t_{th} are the thickness of the membrane and thermometer, respectively, and ρ is the resistivity of the thermometer. For the Pt thermometer, where t/t_{th} and $\rho(T)$ are both constant, FOM=constant and there is no loss of sensitivity upon scaling. For the low temperature a-Nb_ySi_{1-y} thermometers, both t/t_{th} and ρ were varied to optimize the sensitivity while keeping the resistance at a measurable value, typically, <1 MΩ. This will be further discussed in Sec. III.

III. FABRICATION

The thin film nanocalorimeters are fabricated in the UC Berkeley Microfabrication Laboratory on 4 in. (100) silicon wafers using micro electromechanical systems (MEMS) processing techniques with modifications required to protect the thin Si–N before and after releasing the membranes. A 100 nm oxide layer is grown by wet oxidation of both sides of the Si wafer at 1000 °C. This oxide layer reduces the capacitive coupling between the heater, thermometers, and ground through the silicon wafer. The oxide is etched from the back of the wafer using 5:1 buffered HF (BHF) and low stress amorphous Si–N is deposited at 835 °C in a LPCVD furnace using a 4:1 mixture of dichlorosilane and ammonia.

The Si–N on the front surface of the wafer forms the membrane and the Si–N on the back is the mask for the subsequent silicon etch. Scratches in the thin Si–N film will result in unwanted etching of the Si therefore a 200 nm film of Cr is deposited on the back surface of the wafer to protect the Si–N during processing. A Pt film is sputtered onto the front of the wafers where the heaters, thermometers, and leads are lithographically patterned and then etched in aqua-regia at 85 °C. The front surface of the wafer is then protected with photoresist and the Cr film is removed from the backside. The Si–N on the back of the wafer is patterned and etched. The membranes are released by etching the exposed Si in KOH at 80 °C. The top surface oxide layer is removed from the back of the membrane in 5:1 BHF leaving the clean bottom surface of the Si–N as a growth surface for future sample deposition. Vacuum chucks are avoided for the remainder of the processing as the membranes are somewhat fragile. The low temperature a-Nb_ySi_{1-y} thermometers are cosputtered, annealed, patterned, and then etched in an SF_6 plasma. Thicknesses of the Pt, a-Nb_ySi_{1-y}, oxide, and Si–N are measured either with a profilometer or optical reflectometer. A batch consists of 6–18 wafers with each wafer holding 52 devices and yields are typically 85%.

Residual stress is kept below 200 MPa for all films to reduce strain on the membranes. The stress in the LPCVD Si–N depends on the deposition temperature and ratio of dichlorosilane and ammonia precursor gases.[11] The stress in the sputtered Pt and a-Nb_ySi_{1-y} films is controlled by varying the pressure of the argon gas.[14] Film stresses are determined by measuring the Si wafer curvature before and after film deposition with a Tencor FLX-2320.

The resistance of the a-Nb_ySi_{1-y} thermometers is a function of both doping y and annealing temperature T_A.[15] Annealing the devices ensures that they are thermodynamically stable and thus reproducible for sample preparation or measurements below T_A. A device's operating temperature range is determined by the choice of y and T_A. Thermometers with $R \simeq 1$ MΩ at 300 mK can be obtained for $y \simeq 0.1$ when $T_A = 300$ °C. The operating temperature range can be expanded by increasing both y and T_A. Low temperature thermometers have been reliably produced by annealing films with $y \simeq 0.13$ at 500 °C.[15] Figure 2 shows the predicted FOM for the a-Nb_ySi_{1-y} where t/t_{th} and ρ are both held constant. By holding ρ constant and decreasing t/t_{th}, the thermometer resistance increases above 1 MΩ and the FOM decreases. y was increased to compensate for the increased thermometer resistance but this resulted in a decrease in the FOM. The FOM for these thermometers can be further improved by annealing above 300 °C and by decreasing y and increasing t_{th} for future devices.

Samples and conduction layers are vapor deposited onto the small central sample area of the membrane using a micromachined deposition mask. A 5 μm gap between the deposition mask and membrane is used to keep the error in sample area to ≤1% from typical shadowing effects during growth. These deposition masks are fabricated from 6 in. silicon wafers with a nominal thickness of 650 μm. The wafers are coated with 400 nm of Si–N, patterned on the front and back, and etched in KOH at 80 °C. The resulting

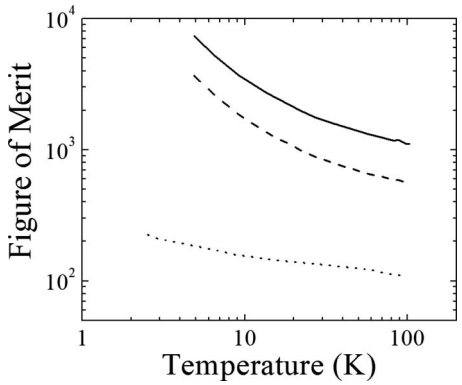

FIG. 2. Low temperature sensitivity FOM=$(t/t_{th})^{1/2}T^{3/2}/\rho^{1/2}d\rho/dT$ of the nanocalorimeter using a-Nb_ySi_{1-y} thermometers. The predicted nanocalorimeter FOM (solid line) which is the same as the microcalorimeter, FOM for $t/t_{th}=1/6$ and ρ=constant (dashed line), and the measured FOM with t/t_{th}=constant and ρ decreased to reduce the thermometer resistance below 1 MΩ.

mesa structure fits in the etch pit on the nanocalorimeter and has a through wafer opening in the center that defines the 1×1 mm^2 sample area. Appropriate choice of convex corner compensation is required to prevent undercutting the mesa structure along the (411) planes that are exposed at the corners. The convex corner compensation method laid out by Fan and Zhang[16] was found to be sufficient for this deposition mask structure.

IV. EXPERIMENTAL METHOD

The nanocalorimeter is either mounted onto a measurement system once the sample and conduction layer are deposited or the device is attached to a sample stage with a deposition mask for *in situ* deposition and measurement. In either case, the device is clamped to a Cu block with a small amount of either Apiezon N or H grease applied to the block to ensure good thermal contact. The device can be operated over a temperature range from 300 mK to 800 K when it is prepared as described above. Electrical connections are made by gold wire bonding to the contact pads on the Si frame. A commercial Cernox thermometer and temperature controller are used to measure and control the temperature of the Cu sample block. During the measurement, each resistance thermometer on the device is calibrated to the temperature of the block thermometer. The resistance of the device sample thermometers typically vary by a small amount for devices from the same wafer. This variation is due to either thickness or, for the a-Nb_ySi_{1-y}, small composition gradients across the wafer. All measurements are made under high vacuum ($<1 \times 10^{-7}$ Torr) to eliminate irreproducibility in c or K from small amounts of gas or ice.

The small ΔT relaxation method[1,8,17] is typically used for heat capacity measurements, however, the nanocalorimeter is compatible with other small sample calorimetry techniques. For this measurement, the thermal link of the calorimeter K is measured by applying a known power P to the heater and then measuring the steady state temperature rise ΔT of the sample area above the Si frame which is held at the temperature of the block T_0. Solution of the steady state heat flow equation gives $K=P/\Delta T$. P is then set to 0 and the subse-

quent exponential temperature decay is recorded as a function of time. The time constant of the temperature decay $\tau = c_T/K$ where $c_T = c_a + c_s$ is the total heat capacity of the calorimeter, sample, and conduction layer.

This simple model for heat flow in the device applies when the sample area is isothermal and both K and c do not change appreciably during the measurement. Temperature gradients in the sample area have been shown to be $<2\%$ when using a conduction layer with a high thermal conductivity, such as Au or Cu, that has at least the same thickness as the membrane.[9] Changes in K and c are kept sufficiently small with the appropriate choice of ΔT. For the steady state measurement of K, ΔT in the range of 1%–10% of T_0 maintains the linearity of K over the temperature interval T_0 to $T_0 + \Delta T$. For the temperature decay, ΔT of 1%–2% of T_0 is used and results in an error in c that is $\leq 0.01\%$. A detailed discussion of this technique along with a comparison to both a one dimensional (1D) model and two dimensional (2D) numerical simulation are reported elsewhere.[1,8,9,17]

To measure ΔT, either the Pt or one of the a-Nb_ySi_{1-y} sample thermometers (depending on temperature T_0) is connected to a lock-in amplifier through an autobalancing bridge which references a matching thermometer on the device's frame (see Fig. 1). The temperature of the block is held stable at T_0, the bridge is balanced, and the resistance of the sample thermometer is measured along with the temperature of the calibrated block thermometer. The bridge is then driven off balance by an amount ΔV when power P is supplied to the sample heater. ΔT of the sample is then determined from the measured $R(T)$ calibration for the sample thermometer.[1,18] For a given T_0, several heater powers are applied corresponding to $\Delta T/2, \Delta T, 3\Delta T/2, 2\Delta T$ to test linearity of K around $T_0 + \Delta T$.

A Signal Recovery model 7265 DSP Lock-in amplifier provides the excitation voltage for the bridge and records the relaxation time constant τ using an internal fast A/D converter. An excitation frequency of several hundred hertz to a few kilohertz is used for measurement of the decay. Between 25 and 100 decays are averaged at a single temperature. The resistance of the a-Nb_ySi_{1-y} sample thermometer is 500 $k\Omega - 1$ $M\Omega$ at low temperatures and this leads to an RC attenuation of the off-null voltage of the bridge for frequencies above ~3 kHz. This attenuation is acceptable for the time dependant measurement as only the time constant of the decay is important but it is unacceptable for K where an accurate measure of ΔV of the bridge is needed to determine ΔT. A low frequency, typically 17 Hz, is therefore used for the steady state measurement to avoid this RC attenuation.

Usually, one nanocalorimeter per wafer is measured (with a conduction layer) to determine c_a for all devices from the wafer. The remaining devices have both a sample and a conduction layer deposited on them. The sample's heat capacity c_s is determined by subtracting the addenda from the total measured heat capacity, $c_s = c_T - c_a$. The small variations in c_a for each device due to differences in Pt and conduction layer thicknesses between the addenda and sample devices are calculated and corrected.

The data presented below are for devices with varying conduction layer thicknesses and materials. The membrane thickness for these nanocalorimeters is 50 nm though devices with 30 nm membranes have been fabricated. Additionally, process variations resulted in the thickness of the Pt heater and thermometers being greater than the desired value from scaling. The increased thickness of Pt increases c_a and the conduction term in K. All measurements were performed in a ^{4}He cryostat over the temperature range 2–300 K. The resistance of the a-Nb_ySi_{1-y} thermometers were successfully measured down to 300 mK in a ^{3}He cryostat. The Pt thermometers were tested up to 800 K in vacuum both by raising the temperature of the sample block and monitoring the resistance of thermometer and also by holding the sample block and silicon frame of the calorimeter at room temperature and heating the sample area of the membrane up to 800 K. For the remainder of the paper, we will refer to the heat capacity of the Si–N membrane, heaters, and thermometers as the addenda and treat the conduction layer as the sample. It should be noted that a measurement of a device without a conduction layer is not meaningful since the isothermal criterion is not satisfied.

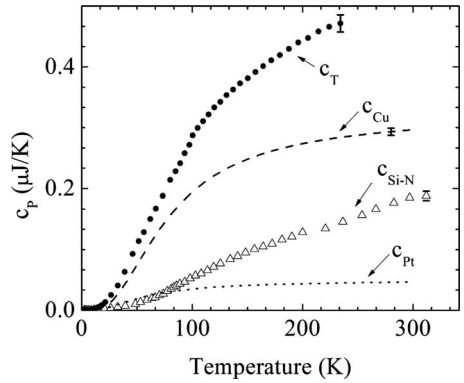

FIG. 3. Total measured heat capacity c_T of a 50 nm thick device with 86.4 nm of Cu [contributions from: Cu conduction layer; Si–N membrane; Pt heater, thermometer, and leads; and a-Nb_ySi_{1-y} thermometers (small and not shown)]. c_{Cu} and c_{Pt} are calculated from bulk data. (Ref. 19) c_{Si-N} is calculated from $c_T - c_{Cu} - c_{Pt}$. (Ref. 12).

V. RESULTS

Figure 3 shows c_T for a device with 86.4 nm thick Cu conduction layer. Also shown are calculated c for each component; Si–N membrane, Pt elements, and Cu conduction layer. The heat capacity of the a-Nb_ySi_{1-y} thermometers is not shown as it makes a negligible contribution.[12] For this sample, the bulk specific heats of Cu and Pt are used to calculate the corresponding thin film contributions which is a reasonable assumption given the results presented below.[19] c_{Cu} is shown for the thickness of Cu in the 1×1 mm^2 sample area. c_{Pt} is a combination of c for all of the Pt in the sample area along with 29% of c for the Pt on the membrane border. This geometric factor for the border contribution is a result from 2D heat flow simulations.[9] The Si–N's heat capacity is calculated from $c_{Si-N} = c_T - c_{Cu} - c_{Pt}$. Knowing each of these contributions allows c_a to be calculated for any device to within 2% as is demonstrated below.

Figure 4 shows the temperature dependence of K, the measured thermal link of the nanocalorimeter, and the various components that contribute to this value. Measurements

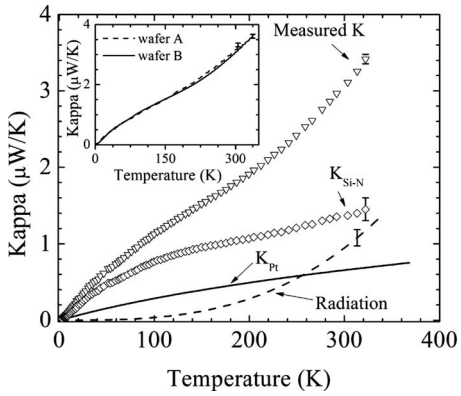

FIG. 4. Measured total thermal link $K=P/\Delta T$ of a 50 nm nanocalorimeter shown with the contributions from Si–N membrane, Pt leads, and radiation. K_{Pt} is calculated using the Wiedemann–Franz law with the measured $\sigma(T)$ of the Pt heater. K_{Si-N} is calculated by subtracting the contributions from Pt leads and radiation. K_{rad} is taken as the T^3 term in $K-K_{Pt}$. (Ref. 12) Inset: K for two devices from different wafers in same process lot.

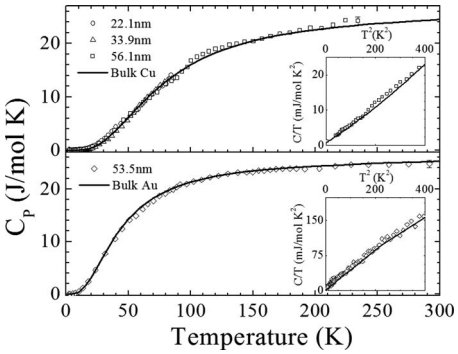

FIG. 5. Specific heat of Cu (a) and Au (b) films of various thicknesses. Bulk values (solid lines) are from Ref. 19. Data in (a) is the difference between devices with thick and thin Cu films. The specific heat of Au (b) was determined as described in the text. Insets: C/T vs T^2 for 56.1 nm Cu (a) and 56.3 nm Au (b).

of K for devices from the same wafer agree to within 3%. The inset in Fig. 4 shows K for devices from wafers A and B that are from the same process lot. Variations in the thickness of the Pt and Si–N account for the difference between the measured K. The thickness differences between wafers for the Si–N and Pt are 1.5% and $\leq$10%, respectively. Correcting for these different thicknesses reduces the variation to $\leq$2% which is within the measurement error.

The contributions to K shown in Fig. 4 were calculated following the procedure detailed in Ref. 10. The thermal conductance of the Pt leads K_{Pt} is calculated from the thermal conductivity given by the Wiedemann–Franz law $(k/\sigma=L_0T)$. The electrical conductivity σ of the Pt is calculated from the measured $R(T)$ of the Pt heater which, along with the thermometers and leads, is lithographically patterned and its geometry well known. K_{Pt} is subtracted from K and the resulting curve is fit to a functional form $a+bT+cT^3$ above 100 K. The cubic term is assumed to be due to the leading term in the radiation contribution $P_{rad}=A_{eff}\epsilon\sigma[(T_0+\Delta T)^4-T_0^4]\approx A_{eff}\epsilon\sigma T^3\Delta T\equiv K_{rad}\Delta T$ with $K_{rad}=A_{eff}\epsilon\sigma T_0^3$. From this we can find the contribution from the Si–N $K_{Si-N}=K-K_{rad}-K_{Pt}$.[12] The contribution from K_{rad} scales as the exposed surface area A_{eff} and is in good agreement with the predicted reduction of x^2.

Heat capacity measurements were also made on 52.5 nm and 30.3 nm thick Cu films and a 54.6 nm Au film. In all cases, the temperature decays were verified to be single exponential over 6τ. The nanocalorimeter for the Au film was from wafer A and the nanocalorimeters for the Cu films were from wafer B. All of the sample films were grown by thermal evaporation at a base pressure of 2×10^{-6} Torr and a deposition rate of 2–5 Å/s. Film thicknesses were monitored during growth with a quartz crystal thickness monitor and verified by measuring the thickness of a neighboring sample with a KLA-Tencor Alphastep IQ surface profilometer. The uncertainty in film thickness is 1.5% for these samples.

Figure 5(a) shows c_s for several thicknesses of Cu. Here we choose to find c_s by taking the difference between τ for each of the measured samples and multiplying the result by an average K for this wafer. This subtraction removes the contribution of c_a and the thinner conduction layer by treating the extra Cu of the thicker layer as the sample, e.g.,

$$c_{Cu}^{33.9\ nm}=c_T^{86.4\ nm}-c_T^{52.5\ nm}$$
$$=K^{86.4\ nm}\tau^{86.4\ nm}-K^{52.5\ nm}\tau^{52.5\ nm}$$
$$=K(\tau^{86.4\ nm}-\tau^{52.5\ nm}),$$

since K for each device was measured to be the same, and similarly for 56.1 nm=86.4−30.3 nm and 22.2 nm =52.5−30.3 nm. The assumption of an average K, and thus c_a, introduces an additional error that depends on small differences in Pt lead thickness for each device. The resulting data are normalized to their molar mass and are in good agreement with the literature values for bulk Cu which is shown as well.[19]

Figure 5(b) shows c_s for a 54.6 nm thick Au film. For this sample, c_a was calculated as described above based on the measured thicknesses of the Si–N and Pt for this wafer compared to wafer B. The specific heat for bulk Au (Ref. 19) is shown and is in good agreement with the measured value. This agreement validates the differential method for measuring heat capacity along with verifying that the extracted heat capacity of the Si–N is correct since $C_{Cu}(T)$ is very different than $C_{Au}(T)$. The agreement of the Cu and Au films with bulk specific heat values also indicates that both electronic and lattice contributions to the specific heat are not changed for films as thin as 30 nm.

We turn now to the intrinsic values of k and C for the Si–N extracted from the measured values of K and c_a.[10] We use the results of 2D heat flow simulations that show how contributions from the membrane border area need to be considered.[9] The intrinsic thermal conductivity of the Si–N $k_{Si-N}=K_{Si-N}/\alpha t$ where t is the thickness of the Si–N and $\alpha=10.33$ is a geometric constant obtained from the simulations, somewhat equivalent to the ratio of the path length to width. The intrinsic specific heat of the Si–N C_{Si-N} is calculated from c_{Si-N}. From the 2D simulations, the effective volume of Si–N is the sum of the central sample area and border contributions, $V_{eff}=\{1\ mm^2+0.24[(2\times2)-(1\times1)]mm^2\}\times50$ nm where 0.24 is a geometric factor taken from the simulations in the limit of a good thermal conduction layer, as here.

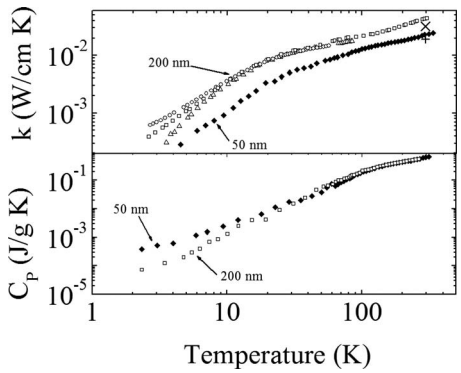

FIG. 6. Thermal conductivity (a) from 50 nm Si–N membranes (filled diamonds) compared to values for 200 nm membranes (squares) grown in the same furnace as the 50 nm membranes and previously reported 200 nm films (circles and triangles.) (Ref. 12) Room temperature values for 200 nm (×) and 50 nm (+) are measured by the 3ω technique. (Ref. 20) Specific heat (b) from 50 nm (diamonds) and 200 nm (squares) Si–N membranes.

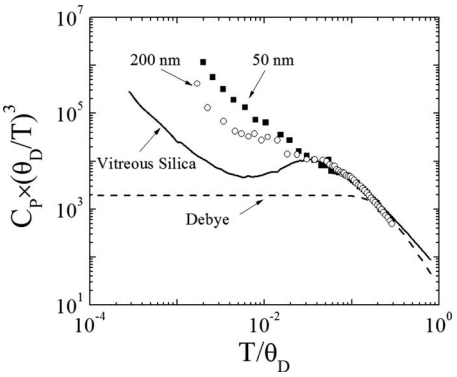

FIG. 7. Reduced specific heat (J mol^{-1} K^{-1}) of silicon nitride (50 nm and 200 nm) and vitreous silica (Ref. 24) plotted as $C_P \times (\theta_D/T)^3$ vs reduced temperature T/θ_D. The dashed line is the Debye specific heat. Debye temperatures were calculated from the measured sound velocities. (Refs. 20, 23, and 24).

Figure 6(a) shows the thermal conductivity of Si–N for a 50 nm and several 200 nm membranes.[10,20] The thermal conductivity for 200 nm membranes below 10 K was reported to be sensitive to the surface roughness of the membrane which is primarily determined by oxide preparation technique.[10] Phonon scattering from the rougher surfaces is believed to be diffuse and leads to a decrease in thermal conductivity. k for the nanocalorimeter's 50 nm membranes is reduced over the entire measured temperature range up to a factor of three when compared to 200 nm membranes prepared under similar conditions. The reduction in k is likely due to boundary scattering of long wavelength phonons from the surfaces of the membrane. Recent thermal conductivity measurements of an a-Si:H film using time-domain thermoreflectance have shown that a large fraction of the room temperature thermal conductivity is due to phonons with wavelengths of several nanometers and mean free paths of hundreds of nanometers.[21] We suggest therefore that boundary scattering in the thinner nitride films reduces the mean free path of the phonons which in turn reduces k over the entire measured temperature range.

Figure 6(b) shows the specific heat (J g^{-1} K^{-1}) of the 50 nm Si–N compared to 200 nm Si–N membranes. Above 20 K, $C_{\mathrm{Si-N}}$ for both samples agrees to within a few percent and rules out any thickness errors that might account for the discrepancy seen in k. Below 20 K, the 50 nm films show an increase in c as compared to 200 nm films.

Rutherford backscattering (RBS) measurements for Si–N films reported here and previously[12] show the stoichiometry to be $SiN_{1.15\pm0.05}$ with ≤ 1 at. % hydrogen as measured by hydrogen forward scattering in agreement with previous results.[22] The density, also determined from RBS, for these films is $\rho = 2.68 \pm 0.07$ g/cm^3. There was no depth dependence to the composition found from the RBS measurements. The index of refraction, which is a measure of film composition and stress, measured by spectroscopic ellipsometry is 2.15 ± 0.05 for all of these films as well.[11] From these measurements, all of the films in Fig. 6 appear to be very similar chemically and it seems unlikely that any remaining small variations in stoichiometry or density would lead to the differences seen in k and C.

Room temperature acoustic measurements on the 50 nm films give the longitudinal speed of sound $v_l = 11.7 \times 10^5$ cm/s which is ~6% larger than v_l for 200 nm thick Si–N.[12,20,23] The previous result from Ref. 23 are corrected here for the measured density. Room temperature measurements of k have been made on 50 nm[20] and 200 nm[12,22] Si–N films using the 3ω technique. These values are systematically 14% lower than the values determined from calorimetry measurements and lie slightly outside of the room temperature 10% error bar in k that is dominated by uncertainty in the model for radiation. All of these differences are negligible compared to the factor of three change in k at all temperatures and the factor of five change in C by 2 K.

Figure 7 shows the specific heat of Si–N plotted as $C_P \times \theta_D/T^3$ versus T/θ_D along with vitreous silica from Ref. 24. Deviations from Debye-like specific heat, such as a linear term below 1 K in C, are commonly seen in amorphous materials.[24] The linear term, which appears as an upturn in C/T^3, is attributed to degeneracies in the amorphous matrix that gives rise to tunneling states and is believed to be universal in all amorphous materials.[25] The linear term in Si–N is appreciable below 6 K in 200 nm films and 20 K in the 50 nm films.[12] The large linear term and high onset temperature are both surprising given that Si–N appears to have a low density of tunneling states, as measured by internal friction, which is well outside of the universal regime.[26,27] Measurements below 2 K are still needed to confirm these results.

From a measurement perspective, the reduction in $k_{\mathrm{Si-N}}$ is beneficial as a decreased thermal conductance leads to increased thermal isolation of the sample. This means that c_a can be reduced by using a thinner conduction layer and still satisfy the isothermal condition for 2% accuracy.[9] However, the increase in $C_{\mathrm{Si-N}}$ below 20 K results in an addenda that is five times larger than expected at 2 K.

VI. CONCLUSIONS

A thin film nanocalorimeter for measuring the heat capacities of 30 nm thin films with ~2% absolute accuracy has been designed, fabricated, and tested. We present heat capac-

ity measurements from 2–300 K; device thermometry has been tested from 300 mK to 800 K. Heat capacities of several Cu and Au films were measured and showed that the nanocalorimeter can be used to measure the heat capacities of films as thin as 30 nm with absolute accuracy $<5\%$, limited by a combination of electrical noise, film thickness uncertainty, and $\leq 2\%$ systematic error from the measurement technique. The specific heat and thermal conductivity of the thin amorphous silicon Si–N membrane have been extracted and compared to data on thicker membranes. k is reduced by approximately a factor of three over the entire temperature range while an increase in C is found below 20 K and is a factor of five at 2 K. The data presented here for amorphous Si–N and recent results for a-Si:H suggest that the current models for amorphous materials may need to be revisited as new measurement techniques such as this allow investigations of materials not available for bulk measurement techniques. When scaling down the thin film calorimeter, it was necessary to optimize the electrical and thermodynamic response of the device around the strength of the supporting Si–N membrane. It is possible to further reduce the size of the calorimeter, however, the ability to reliably make ultrathin membranes will determine the lower limit on the membrane thickness and, thus, set a lower bound on the heat capacity of the calorimeter.

ACKNOWLEDGMENTS

We thank David Cahill for the room temperature sound velocity and thermal conductivity measurements, Kin Man Yu for the RBS results, Chloé Baldasseroni, Zoe Boekelheide, David Cooke, Erik Helgren, Xiao Liu, and Barry Zink for helpful discussions, and the students and staff at the UC Berkeley Microlab for assistance with this project. This work was supported by the Director, Office of Science, Office of Basic Energy Sciences, Materials Sciences and Engineering Division, of the US Department of Energy under Contract No. DE-AC02-05CH11231.

[1] D. W. Denlinger, E. N. Abarra, K. Allen, P. W. Rooney, S. K. Watson, and F. Hellman, Rev. Sci. Instrum. **65**, 946 (1994).
[2] S. L. Lai, G. Ramanath, L. H. Allen, P. Infante, and Z. Ma, Appl. Phys. Lett. **67**, 1229 (1995).
[3] K. Allen and F. Hellman, J. Chem. Phys. **111**, 5291 (1999).
[4] D. Kim, B. L. Zink, F. Hellman, and J. M. D. Coey, Phys. Rev. B **65**, 214424 (2002).
[5] David W. Cooke, K. J. Michel, and F. Hellman, Rev. Sci. Instrum. **79**, 053902 (2008).
[6] S. L. Lai, J. Y. Guo, V. Petrova, G. Ramanath, and L. H. Allen, Phys. Rev. Lett. **77**, 99 (1996).
[7] S. L. Lai, G. Ramanath, L. H. Allen, and P. Infante, Appl. Phys. Lett. **70**, 43 (1997).
[8] B. Revaz, B. L. Zink, and F. Hellman, Thermochim. Acta **432**, 158 (2005).
[9] B. Revaz, D. O'Neil, L. Hull, and F. Hellman, Rev. Sci. Instrum. **74**, 4389 (2003).
[10] B. L. Zink and F. Hellman, Solid State Commun. **129**, 199 (2004).
[11] M. Sekimoto, H. Yoshihara, and T. Ohkubo, J. Vac. Sci. Technol. **21**, 1017 (1982).
[12] B. L. Zink, B. Revaz, J. J. Cherry, and F. Hellman, Rev. Sci. Instrum. **76**, 024901 (2005).
[13] The FOM is the response of the bridge to a given ΔT. The bridge response $\Delta V \propto I_{\mathrm{th}} \Delta R$. The choice of I_{th} is a compromise between the signal-to-noise ratio and errors from the $I_{\mathrm{th}}^2 R$ self heating in the thermometers (Ref. 18). In the small ΔT method, $P = K \Delta T$ so that $I_{\mathrm{th}} = (K \Delta T_{\mathrm{sh}} / R_{\mathrm{th}})^{1/2}$. The off-null voltage of the bridge can then be written as $\Delta V = (K \Delta T_{\mathrm{sh}} / R_{\mathrm{th}})^{1/2} \Delta T \, \mathrm{d}R/\mathrm{d}T$. Both ΔT and ΔT_{sh} are constants during the measurement and proportional to T. Thus, the figure of merit FOM $= (t_m / t_{\mathrm{th}})^{1/2} T^{3/2} / \rho^{1/2} \mathrm{d}\rho / \mathrm{d}T$.
[14] D. W. Hoffman, J. Vac. Sci. Technol. A **12**, 953 (1994).
[15] D. Querlioz, E. Helgren, D. R. Queen, F. Hellman, R. Islam, and D. J. Smith, Appl. Phys. Lett. **87**, 221901 (2005).
[16] W. Fan and D. Zhang, J. Micromech. Microeng. **16**, 1951 (2006).
[17] R. Bachmann, F. J. DiSalvo, T. H. Geballe, R. L. Greene, R. E. Howard, C. N. King, H. C. Kirsch, K. N. Lee, R. E. Schwall, H. U. Thomas, and R. B. Zubeck, Rev. Sci. Instrum. **43**, 205 (1972).
[18] Typically, $\Delta T_{\mathrm{sh}} = I_{\mathrm{th}}^2 R / K$ is kept below 0.03%–0.1% of T_0 to minimize the error in the temperature calibration of the sample thermometer. Variations in ΔT_{sh} over the temperature interval ΔT lead to errors in K and τ. The error in K is proportional to $I_{\mathrm{th}}^2 dR/dT$ and is $<0.02\%$ for the a-$\mathrm{Nb}_x\mathrm{Si}_{1-x}$ and $<0.01\%$ for the Pt thermometer for a typical $\Delta T < 2\% T_0$. A self-heating correction to the time dependent measurement can be made as well, $\tau = C/(K - \alpha P_{\mathrm{sh}})$ where $\alpha = d \ln R / dT$. For $\Delta T < 2\% T_0$, this correction is negligible: $\alpha P_{\mathrm{sh}} / K \leq 1 \times 10^{-5}$ (Ref. 17).
[19] Y. Touloukian, *Thermophysical Properties of Matter* (IFI/Plenum, New York, 1970), Vol. 4.
[20] D. G. Cahill, personal communication; See for measurement technique, T.-Y. Lee, K. Ohmori, C.-S. Shin, D. G. Cahill, I. Petrov, and J. E. Greene, Phys. Rev. B **71**, 144106 (2005).
[21] X. Liu, J. L. Feldman, D. G. Cahill, R. S. Crandall, D. M. Bernstein, N. Photiadis, M. J. Mehl, and D. A. Papaconstantopoulos, Phys. Rev. Lett. **102**, 035901 (2009).
[22] C. H. Mastrangelo, Y.-C. Tai, and R. S. Muller, Sens. Actuators, A **23**, 856 (1990).
[23] S. Wenzel, Ph.D. thesis, University of California, 1992.
[24] R. C. Zeller and R. O. Pohl, Phys. Rev. B **4**, 2029 (1971).
[25] *Topics in Current Physics*, edited by W. Phillips (Springer, Berlin, 1981), Vol. 24.
[26] X. Liu, T. H. Metcalf, Q. Wang, and D. M. Photiadis, Mater. Res. Soc. Symp. Proc. **989**, A22 (2007).
[27] R. O. Pohl, X. Liu, and E. Thompson, Rev. Mod. Phys. **74**, 991 (2002).